Nanoparticles of iron(II) spin-crossover

Thibaut Forestier,[a] Stéphane Mornet,[a] Nathalie Daro,[a] Taishi Nishihara,[b] Shin-ichiro Mouri,[b] Koichiro Tanaka,[b] Olivier Fouché,[c] Eric Freysz[c] and Jean-François Létard*[a]

Received (in Cambridge, UK) 16th April 2008, Accepted 2nd June 2008
First published as an Advance Article on the web 16th July 2008
DOI: 10.1039/b806347h

We report the synthesis of spin crossover 69 nm spherical nanoparticles of $[Fe(NH_2\text{-}trz)_3](Br)_2{\cdot}3H_2O{\cdot}0.03$(surfactant) ($NH_2$trz = 4-amino-1,2,4-triazole, surfactant = Lauropal), prepared by the reverse micelle technique, which exhibit at room temperature a thermal hysteresis characterized by magnetic, diffuse reflectivity and Raman studies.

Multifunctional molecular materials with tuneable properties under external stimuli like temperature, light irradiation or pressure, through the spin crossover (SCO) phenomenon offer some promising opportunities for applications in information processing, sensors and/or displays devices.[1] Some of these materials are already known to display abrupt transitions with large hysteresis loops centred at room temperature.[2] That confers to this class of system a memory effect suitable for data storage where each of the two spin states can be associated to a binary digit with respect to the magnetic response (diamagnetic low spin/paramagnetic high spin in the case of iron(II) complexes) and/or the thermochromic optical properties.[2,3]

One of the main challenges for chemists with regard to the design of molecular-based memory devices is the control of the size of the SCO clusters that exhibit a thermal hysteresis loop. The size available to date is far from the level of miniaturisation required for the realisation of nanoscale processors.[3] To reach this goal, the use of both the top-down and the bottom-up approaches can be envisaged. Concerning the former method, the production of fine particles requires grinding and sieving steps which are not desirable for the SCO phenomenon. When a mechanical stress is exerted on coordination compounds in the solid state, a molecular distortion results and the SCO behaviour irreversibly changes; *e.g.* residual HS fraction at low temperature.[4] An elegant top-down approach currently developed by the Bousseksou group consists of preparing micro- and nanometer-sized patterns of the SCO material using a combination of lift-off and multilayer sequential assembly methods.[5]

[a] *ICMCB, CNRS, Université Bordeaux 1, 87 Av. Doc. A. Schweitzer, F-33608 Pessac, France. E-mail: letard@icmcb-bordeaux.cnrs.fr; Fax: +33(0)540002649; Tel: +33(0)540002679*
[b] *Dept. of Physics, Graduate School of Science, Kyoto University, Sakyo, Kyoto 606-8502, Japan. E-mail: kochan@scphys.kyoto-u.ac.jp*
[c] *Centre de Physique Moléculaire Optique et Hertzienne, UMR CNRS 5798, Groupe Photophysique des Systèmes Moléculaires, Université Bordeaux I, 351 Cours de la Libération, 33405 Talence cedex, France*

Concerning the bottom-up approach, many efforts have been dedicated to the step-by-step synthesis. This challenging strategy is particularly promising since each synthetic step can be precisely controlled. Examples of dinuclear,[6] trinuclear[7] and tetranuclear[8] SCO systems, with cooperative and/or anti-cooperative interactions between the metal centers, have been described in the literature. An alternative route to synthesize a nanoscopic SCO material is based on the use of water-in-oil (w/o) emulsions to confine the growth of the coordination network.[3,9] Mann and co-workers were the first to apply the reverse micelles technique to the preparation of nanoparticles of a Prussian Blue analogue.[10] With this method, they obtained nanocrystals stabilized within micelles with a size ranging from 12 to 50 nm. Later, Catala *et al.*,[11] by adapting the chemical conditions, reported Cr^{III}–Ni^{III} cyanide-bridged magnetic particles with a size distribution of 3 nm.

In this communication, we show that the reverse micelle technique can be also adapted to prepare well-defined nanoparticles of iron(II) SCO materials. The dispersed water droplets act as microreactors where chemical reactions can be performed to generate the required product in the form of a colloidal dispersion. For that we have selected the 4-amino-1,2,4-triazole (NH_2trz) ligand and prepared $[Fe(NH_2trz)_3](Br)_2$ nanoparticles. At the macroscopic scale, this family of iron(II) SCO coordination polymers is known for exhibiting interesting magnetic properties with a spin transition at room temperature and a well-defined thermal hysteresis.[2,12]

Basically, a reverse micelle is a dispersion of water droplets in a continuous oil phase. In our case, the selected non-ionic Lauropal (Ifralan D0205) of the polyoxyethylenic family plays both the role of surfactant and organic solvent. The first step of the synthesis (Scheme 1) consisted of the dissolution of the reactants: *i.e.* on the one hand the ligand (NH_2trz) and on the other hand the iron(II) salt.† Then at 50 °C the surfactant was added and the two flasks were shaken by dynamic agitation with a vortex system in order to form the thermodynamically unstable reverse micelles (Scheme 1). The two reverse micelle systems were then mixed and the dynamic vortex maintained for 5 min to support the micellar exchange. Immediately after that diethyl ether solvent was added to break down the emulsion and limit molecular diffusion degradation. Indeed, the diethyl ether solvent dissolves the surfactant without denaturising the iron(II) coordination polymer, which finally precipitates. This was followed by a series of extraction-washing steps to obtain the final powder. Further purification was performed by the Soxhlet technique to reduce as far as

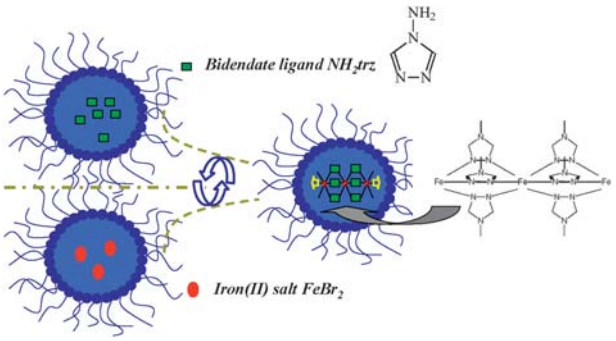

Scheme 1 Synthetic route and schematic representation of the $Fe(NH_2\text{-trz})_3$ unit.

possible the presence of residual surfactant. Elemental analysis on the powder was consistent with the general formula $[Fe(NH_2\text{-trz})_3](Br)_2{\cdot}3H_2O{\cdot}0.03$(surfactant). Transmission electron microscopy (TEM) images (Fig. 1) of particles dispersed in an ethanol solution, after solvent evaporation, showed a rather good distribution of spherical particles centred at 69 nm. Spherical particles were obtained because the synthesis of the polymeric structure has been made in nano-droplets which limits the size of complex and predetermine its form.

Fig. 2 compares the thermal spin transition measured for a collection of nanoparticles and for macroscopic particles of typically few micrometers in both the cooling and warming modes. This behaviour was independent of the number of heating–cooling cycles. The magnetic response was expressed in the form of the $\chi_M T$ *vs.* T curves, where χ_M is for the molar magnetic susceptibility and T the temperature. At high temperature (*i.e.* 360 K), $\chi_M T$ of the nanoparticles is equal to 3.1 cm^3 K mol^{-1}, as expected for a quintet iron(II) complex in a HS state ($t_{2g}^4 e_g^2$, $S = 2$). On cooling, $\chi_M T$ abruptly decreases at $T_{1/2}\downarrow$ = 303 K, falling to 0.4 cm^3 K mol^{-1} at 280 K. No further change appears at lower temperature, suggesting that approximately 15% of the material remains in its HS state after cooling. Such a magnetic residual at lower temperatures is often observed in this kind of material and is attributed to the external iron(II) chain, saturated by water ligands instead of nitrogen atoms of the triazole group. The ligand field of the iron(II) metal ion is consequently weakened, favouring the HS state at all temperatures. This kind of difference of ligand field has been for example reported for iron(II) trinuclear oligomers.[7] On the warming mode, at $T_{1/2}\uparrow$ = 311 K, the LS → HS transformation occurs, showing the presence of a thermal hysteresis of about 8 K. These

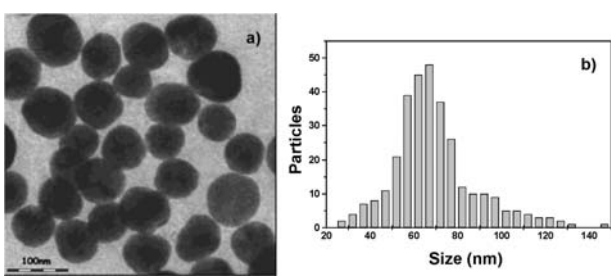

Fig. 1 (a) TEM image of $[Fe(NH_2\text{-trz})_3](Br)_2{\cdot}3H_2O{\cdot}0.03$(surfactant) nanoparticles prepared by a reverse micelle method. (b) Statistic distribution evaluated according to TEM images on around 300 particles, average size 69 nm, minimum and maximum sizes, 26 and 147 nm, respectively, disparity 19 nm.

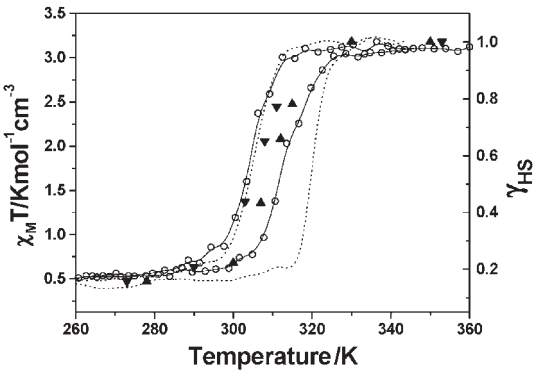

Fig. 2 Plot of $\chi_M T$ *vs.* T of $[Fe(NH_2trz)_3](Br_2){\cdot}3H_2O{\cdot}0.03$(surfactant) for nanoparticles (—) and for macroscopic particles obtained from a typical synthesis (--). The iron(II) HS molar fraction, γ_{HS}, is directly deduced from the $\chi_M T$ product through $\gamma_{HS} = \chi_M T/(\chi_M T)_{HT}$ where $(\chi_M T)_{HT}$ is the high-temperature limit, typically at 360 K. The black triangles represent the calculated HS fraction obtained from the Raman spectrum at low frequency, *i.e.* 244 cm^{-1}, characteristic of the vibration of the inner Fe–N coordination sphere for the LS state.

SCO properties are very similar to those of the macroscopic particles, with the exception of the thermal hysteresis width, which appears to be less pronounced (Fig. 2).

The thermal spin-crossover regime has been also monitored by following the visible spectrum of the sample as a function of temperature, measured by diffuse absorption. At the macroscopic scale, iron(II) triazole polymers present a pronounced thermochromism upon the spin transition, with an absorption band around 520 nm in the purple LS state attributed to the $^1A_{1g} \rightarrow {}^1T_{1g}$ d–d band and an absorption of lower energy in the near infrared (830 nm) in the uncoloured HS state due to the $^5T_{2g} \rightarrow {}^5E_g$ transition. The temperature dependence of the reflectivity signal is in perfect agreement with the magnetic properties of Fig. 2 and confirms that the pink/white colour change *vs.* temperature observed for the nanoparticles reflects the occurrence of a SCO transition with a well defined hysteresis at room temperature.

To complete this analysis, Raman studies have been performed on an assembly of these nanoparticles. Indeed the change in metal-to-ligand bond distance is known to significantly affect the force constant (f) of the vibrations and particularly the low-frequency region, characteristic of the Fe–N vibration modes. On the macroscopic scale, Smit *et al.*[13] described the presence of a characteristic Fe–N stretching vibration for the LS state at 244 cm^{-1} for the analogous iron(II)triazole polymer complex $[Fe(NH_2trz)_3](ClO_4)_2$. Interestingly, for the HS → LS transformation that occurs on cooling for nanoparticles, we also clearly noticed a growing peak at 244 cm^{-1}. By increasing the temperature this peak decreases until disappearing completely (Fig. 3). Fig. 2 shows the intensity of this peak *vs.* temperature (*i.e.* the HS fraction *vs.* temperature), and is in good agreement with the magnetic data.

Finally, in order to highlight the presence of amino groups on the surface of the TS particles and prove their availability for grafting with other nanoparticles in a near future, we have tested the ability of coating gold nanoparticles. Two different strategies were used; (i) the first route consists of using the negative charge of carboxylated gold clusters[14] to

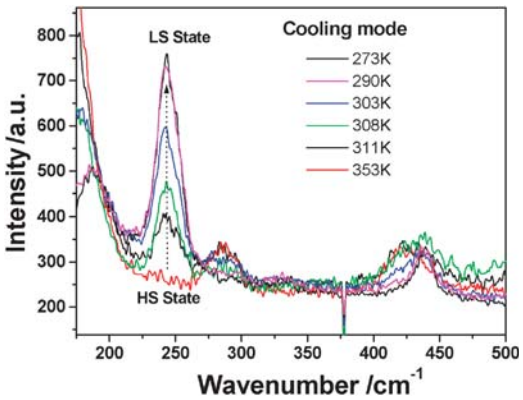

Fig. 3 Temperature-dependent Raman spectra of a collection of nanoparticles recorded using 514.5 nm excitation (Coherent Ar^+ laser, at 8.1 mW cm^{-2}).

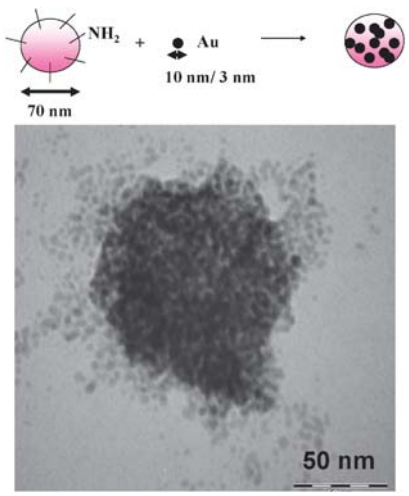

Fig. 4 TEM image of $[Fe(NH_2\text{-trz})_3](Br)_2{\cdot}3H_2O{\cdot}0.03$(surfactant) nanoparticles coated with gold particles of 3 nm.

electrostatically interact with the protonated amino groups of TS particles in solution, and (ii) the second approach is based on the ligand exchange properties of weakly adsorbed polymer macromolecules on the gold surface by the amino groups of the TS particles.‡ In both cases, the TEM images show that clusters and gold nanoparticles are intimately adsorbed on the TS particle surface with a high density of coating, as illustrated in Fig. 4 for gold nanoparticles of 3 nm.

In conclusion we report the preparation of nanoparticles of a SCO material with a controlled size and shape. In contrast to previous work,[9c] the sharp spin transition and the hysteresis loop for the 69 nm nanoparticles are reminiscent of the bulk powder material.

By using a reverse micellar method with such control over particle size, new opportunities can be explored: other nanoparticles of iron(II) SCO materials are currently being synthesized, with new nanoscale materials explored by grafting organic or inorganic matrices.

GDRI France-Japan, ANR Fast-switch (NT05-3_45333), GIS 'Matériaux en Aquitaine' and the Aquitaine Region are gratefully acknowledged.

Notes and references

† The elaboration of the nanoparticles consists of preparing two solutions: (i) an iron(II) salt $FeBr_2$ (230 mg; 1.07 mmol) in demineralised water (0.8 g) with a trace amount of ascorbic acid and (ii) the amino triazole (270 mg; 3.21 mmol) in demineralised water (0.8 g). Anal. Calc. for $[Fe(NH_2\text{-trz})_3](Br)_2{\cdot}3H_2O{\cdot}0.03C_{20}H_{42}O_6$: C, 14.85; H, 3.65; N, 31.48; Found: C, 14.85; H, 3.39; N, 31.52%.

‡ For adsorption on carboxylic acid-terminated gold clusters, TS particles are suspended in ethanol at a concentration of 10 mg mL^{-1} by the use of a sonicator bath. The solutions are left to incubate overnight without stirring. The sediments were then deposited on a carbon coated copper grid for TEM characterization. Carboxylic acid-terminated gold clusters were prepared by the two-phase reduction method[14] in the presence of lipoic acid.[15] The procedure can be briefly described as follows: 3 mL $KAuCl_4$ 30 mM aqueous solution is transferred to 8 mL of toluene in presence of 50 mM tetra-*n*-octylammonium bromide. Auric salts are then reduced with 2.5 mL of 0.4 M aqueous sodium borohydride. Gold nanoparticles prepared by this method have a narrow size distribution with a particle diameter of 3.1 nm (determined by transmission electron microscopy, TEM). Nanoparticle functionalization is carried out by overnight incubation in a toluene solution containing 0.1 M lipoic acid. The carboxylated nanoparticles are not stable in toluene and can be separated by centrifugation, and washed several times with toluene and once with 1-propanol to remove reaction byproducts. After the final centrifugation, a volume of 5 mL of milliQ water is added and the peptization of the carboxylated gold nanoparticles is performed by adding a few drops of 1 M NaOH solution. The volume of the gold sol is then adjusted to 20 mL with 20 mM Hepes buffer at pH 7.4 (final particle concentration = 2.94×10^{18} particles L^{-1}).

1 See, for general reviews: *Spin Crossover in Transition Metal Compounds*, ed. P. Gütlich and H. A. Goodwin, *Topics in Current Chemistry*, Springer Verlag, Berlin-Heidelberg-New York, 2004, vols. 233–235; P. Gütlich, A. Hauser and H. Spiering, *Angew. Chem., Int. Ed. Engl.*, 1994, **33**, 2024–2054.
2 O. Kahn and C. J. Martinez, *Science*, 1998, **279**, 44; P. Gütlich, Y. Garcia and T. Woike, *Coord. Chem. Rev.*, 2001, **219–221**, 839–879.
3 J.-F. Létard, P. Guionneau and L. Goux-Capes, *Top. Curr. Chem.*, 2004, **235**, 221–249.
4 M. S. Haddad, W. D. Federer, M. W. Lynch and D. N. Hendrickson, *Inorg. Chem.*, 1981, **20**, 131–139.
5 S. Cobo, G. Molnar, J. A. Real and A. Bousseksou, *Angew. Chem., Int. Ed.*, 2006, **45**, 5786–5789; G. Molnar, S. Cobo, J. A. Real, F. Carcenac, E. Daran, C. Vieu and A. Bousseksou, *Adv. Mater.*, 2007, **19**, 2163–2167.
6 J. A. Real, A. B. Gaspar, M. C. Muñoz, P. Gütlich, V. Ksenofontov and H. Spiering, *Top. Curr. Chem.*, 2004, **233**, 167–193.
7 J. J. A. Kolnaar, G. van Dijk, H. Kooijman, A. L. Spek, V. G. Ksenofontov, P. Gütlich, J. Haasnoot and J. Reedijk, *Inorg. Chem.*, 1997, **36**, 2433–2440.
8 M. Ruben, E. Breuning, J.-M. Lehn, V. Ksenofonotv, F. Renz, P. Gütlich and G. B. M. Vaughan, *Chem.–Eur. J.*, 2003, **9**, 4422–4429.
9 J.-F. Létard, N. Daro and O. Nguyen, *Fr. Pat.*, FR 0512476 (2005-08-12) J.-F. Létard, N. Daro and O. Nguyen, *Int. Pat.*, WO 2007/065996 (2007-06-14) E. Coronado, J. R. Galán-Mascarós, M. Monrabal-Capilla, J. García-Martínez and P. Pardo-Ibáñez, *Adv. Mater.*, 2007, **19**, 1359–1361.
10 S. Vaucher, M. Li and S. Mann, *Angew. Chem., Int. Ed.*, 2000, **39**, 1793–1796.
11 L. Catala, T. Gacoin, J.-P. Boilot, E. Rivière, C. Paulsen, E. Lhotel and T. Mallah, *Adv. Mater.*, 2003, **15**, 826–829.
12 O. Kahn, J. Kröber and C. Jay, *Adv. Mater.*, 1992, **4**, 718–728.
13 E. Smit, B. Manoun and D. de Waal, *J. Raman Spectrosc.*, 2001, **32**, 339–344.
14 M. Brust, M. Walker, D. Bethell, D. J. Schiffrin and C. J. Kiely, *J. Chem. Soc., Chem. Commun.*, 1995, 1655–1656.
15 J. M. Abad, S. F. L. Mertens, M. Pita, V. M. Fernandez and D. J. Schiffrin, *J. Am. Chem. Soc.*, 2005, **127**, 5689–5694.